A Localized Surface Plasmon Resonance-Based Portable Instrument for Quick On-Site Biomolecular Detection

S. Rampazzi, G. Danese, *Member, IEEE*, F. Leporati, *Member, IEEE*, and F. Marabelli

***Abstract*—In recent years, several approaches have been developed to carry out biosensors based on Localized Surface Plasmon Resonance (LSPR). However, the high costs of nanostructure fabrication and the absence of autonomous portable devices strongly limit the extensive use of LSPR biosensors outside research laboratories.**

We designed, implemented and tested a novel low cost, multiparametric stand-alone LSPR imaging instrument for biosensing applications. This compact device (15 x 6 x 17 cm size and < 500g weight) consists of a nanohole array biochip integrated with a microfluidic layer and a processing system. An optical apparatus focuses a light beam from an IR LED source and a digital image sensor captures the reflected light from the biochip surface. The signals are processed by the embedded ARM processor and shown on a touchscreen display by a user-friendly application, without the need for other external computational devices.

Moreover, we propose an extremely simple analytical method to reduce image noise without any sophisticated temperature control or external luminosity change compensation.

The device sensitivity of 6 x 10^{-5} Refractive Index Unit (RIU) was measured using glycerol solutions with different concentrations. We demonstrated the efficiency of our system in biomolecular detection by monitoring the Ab-PTX3 antibody in a test that showed the **instrument's potentialities in** the **detection of antibodies. These results confirmed the potential usefulness of the proposed system in several biomedical applications such as medical diagnostic procedures, immunoassays or fast in-loco preliminary analyses without the aid of specialized laboratory or trained personnel.**

***Index Terms* — Localized Surface Plasmon Resonance, biosensors, biomedical instrumentations, portable embedded systems, digital signal processing, ARM processors, optic imaging, bioassay measurements.**

Manuscript received February 10, 2015; revised June 17, 2015; accepted July 15, 2015. Date of publication ???, 2015; date of current version July 28, 2015..

S. Rampazzi, was with University of Pavia, Pavia, IT 27100 Italy. She is now with Positech, via De Amicis 49, Milan, IT 20123 Italy (e-mail: sara.rampazzi@gmail.com).

G. Danese and F. Leporati are with the Electrical, Computer and Biomedical Engineering Department, University of Pavia, via Ferrata 5, IT 27100 Pavia, Italy, (e-mail: {giovanni.danese, francesco.leporati}@unipv.it).

F. Marabelli is with the Physics Department of the University of Pavia, via Bassi 6, IT 27100, Pavia, Italy, (e-mail: franco.marabelli@unipv.it).

I. Introduction

In the past decade, huge developments in nanotechnology pushed researchers to extend their use in a variety of applications and fields. In particular, studies in nanomaterial properties generated new techniques to induce Surface Plasmon Resonance (SPR) phenomena in nanostructures [1]. Several advantages derived from the use of this new approach: the miniaturization of the SPR system, the possibility to perform several experiments on a single surface (SPR *imaging* - SPRi) and an ultrahigh spatial resolution, because every single nanoparticle can be used as an individual transducer for micro-volume samples.

Nevertheless LSPR biosensors are not extensively used outside research laboratories. The reason lies in two main aspects of their production. First of all the high costs of nanostructure fabrication: complex and nonstandard techniques are used to reach an optimal design and an augmented sensitivity; furthermore, the lack of portable stand-alone devices that do not require an external computation device (like a PC) to elaborate the signals.

Several research works concentrated only on increasing LSPR sensitivity by studying the geometry of nanostructures integrated with microfluidic chips [2-5]. Less attention has been devoted to develop an autonomous, portable, mass-producible device for real-time biosensing applications that can be operated without the aid of specialized research laboratories or trained personnel.

In this paper we describe how we designed, implemented and tested a novel stand-alone cheap portable LSPR imaging biosensor (LSPRi) so as to show its very effective sensitive capability [6]. This multi-parametric system detects the presence and measures the amount of specific target molecules in liquid samples and monitors biological and molecular interactions.

The light reflected from the nanostructured surface irradiated at a specific wavelength is acquired by a digital image sensor and processed by the on-board elaborating system.

More than 100 micro-spots of antibodies sensitive to different analytes can be deposited on the surface of the current release of the biochip.

Presence and concentration of the target analytes appear on a touchscreen display and can be stored into a MicroSD memory card in about 12 seconds.

This paper's novelty concerns the design and realization of the electronic support and software interface between the biosensor component and the end-user.

This paper details the prototype of a portable autonomous low-cost and low-power-consumption LSPRi biosensor together with its ARM-based acquisition unit. We present a software platform, conceived for a minimal Linux kernel-based Operating System implementation, that can manage image acquisition and processing.

The impact of external noise on the acquired images' quality was minimized by means of a suitable filtering integrated with the analyte detection algorithm that is illustrated in the following sections.

Finally, we assessed the instrument's sensitivity by measuring the refractive index change in glycerol solutions at different concentrations.

Furthermore, its capability to detect organic molecules was demonstrated by measuring the Ab-PTX3 antibody level in liquid samples. The case studies presented in the paper demonstrate the functionality of the biosensor in terms of sensitivity and accuracy and its potentialities in the performance of assays *in loco* in several biochemical and chemical applications, e. g. to detect toxins and pathogens in water, to control industrial processes or to analyze food analysis and monitor the presence of allergens.

II. SPR AND LSPR BIOSENSORS PRINCIPLES

Surface Plasmons (SP) are coherent oscillations of the free conduction electrons at the interface between two media with different dielectric constants (as a metal and a dielectric) [7]. The optical excitation of surface plasmons is induced by coupling with a light beam at a specific incidence angle and wavelength. The resonant effect thus generated is observable in the reduced intensity of reflected light correlated with the changes in the metal surface's refractive index.

Biosensors that exploit plasmonic resonance use specific molecules immobilized on the metal surface (e. g. antibodies) that react with the target substances (called analytes) diluted in a liquid sample. The receptor-analyte reaction changes the refractive index of the medium, thus altering the resonance conditions.

By means of this label-free technique it is possible to detect molecular bindings directly and in real time, so as to determine the analytes' concentration during this interaction without fluorescence or radioisotope labeling, and to monitor reaction kinetics.

The most common SPR biosensors are typically based on Kretschmann's configuration, in which a laser or a LED light source radiates a dielectric (often glass) prism covered with a thin metal layer. Their sensitivity can reach about 10^{-8} RIU [8]; however, some difficulties are associated with the optimization of these devices' performances. In fact, the effect of SPR phenomena depends highly on the thickness of the metal film and on the geometrical parameters and kind of materials used in the construction of the prism [9].

The same configuration can be applied in the case of waveguide coupling-based SPR biosensors, such as fiber-optic ones. The waveguide is usually coated with a planar metal layer onto which the receptors are immobilized. The injected light propagates through the medium and induces SPR at the interface between the metal and the waveguide [10].

In the case of optical fibers, the fiber core is deprived of its the silicon cladding and coated with a metal layer surrounded by a layer of receptors. As for prism configuration, these solutions require a careful choice of the fiber type and materials to be used.

The high sensitivity of SPR traditional biosensors is in part due to the long decay length of surface plasmons. However, this parameter decreases significantly for the thin analyte layers (5-10 nm biomolecules dielectric monolayers) typical of many biological applications [11]. Another limitation is the fact that temperature fluctuation significantly affects SPR response [12].

In Localized Surface Plasmon Resonance (LSPR) the electrons' oscillations are trapped within conductive nanoparticles or nanoholes smaller than the wavelength of the source beam employed. In this case, the sensitivity of the refractive index change strongly depends on the type of metal, the shape, the size and the distance between the nanostructures [13].

In 2012 Zalyubovskiy and his team demonstrated that the sensitivity of traditional SPR systems is better than that of LSPR biosensors when a gold film with a $\geq$ 20 nm thick analyte layer is used. However, the sensitivity of LSPR devices becomes comparable to that of SPR systems for thin ($\leq$ 10 nm) analyte layers, while remaining less influenced by temperature fluctuations [11].

Many researchers investigated different designs and materials to improve LSPR sensitivity and push its limits of detection [14]. In 1998 the experiments of Ebbesen et al. showed a much higher response in transmitted light intensity in nanohole arrays distributed on thin metal films (called *Extraordinary Optical Transmission* - EOT effect) than in nanoparticle arrays. This behaviour indicates that LSPR nanoholes are, in general, more suitable for a high-sensitivity analysis of molecular adsorption on thin analyte layers [15].

III. RELATED WORKS

Up to the last decade the majority of commercially available SPR biosensors were conceived for laboratory use, and their destination clearly showed limits in terms of costs, size, complexity and portability. Recent years have seen an increasing effort toward the fabrication of compact instruments due to a growing demand of compact multiparametric systems with high sensitivity and low costs.

One of the first available compact SPR sensors is the Spreeta, designed by Texas Instruments. The most famous model, Spreeta 2000, consists of a plastic prism assembled on a PCB that contains an 830 nm IR LED, a Diode Array Detector (DAD) and a flash memory [16]. The light beam goes through a polarized plastic sheet and strikes a glass chip coated with a gold layer. The SPR waves thus produced are captured by the

DAD and the resulting signal is transmitted via a USB interface. A Spreeta costs about 50$ [17]; it has a good resolution (about $5x10^{-6}$ RIU) and three detection channels. However, it must be integrated with external fluidics and processing systems. Another limitation of the Spreeta is that temperature significantly affects its measurements, and a control system is consequently required to keep it under control.

Many research works exploit Spreeta technology to develop multi-analyte SPR biosensors. For example, in 2007 Chinowsky described an instrument made of up to eight 3-channel Spreeta devices assembled with a DSP microcontroller for sensor management and temperature control, a microfluidic system and an LCD display. This semi-automatic lunch-box system is used for toxin, bacteria and virus detection [18].

Hu et al., in 2009, described another device made up of a tree-channel Spreeta that uses three different processors for temperature, data and display control [19]. Both devices have a weight (about 3 Kg and 8 Kg, respectively) that hampers their portability. Also, both can only detect a limited number of analytes: 24 and 3, respectively, including the channel used as control baseline.

Other works focus on the optimization of Kretschmann-based techniques. For example, Cai et al., in 2010, designed an autonomous device based on an image scanner chip in which a wedge-shaped laser beam radiated a cylinder prism. The reflected light was captured by a CCD camera and elaborated by an on-board industrial PC [20]. The sensitivity of the system was about 6×10^{-5} RIU, but each analysis required 30 minutes for baseline stabilization.

Shin et al. developed a similar device using rotating mirrors instead of prism in 2010. A gold chip is irradiated by a diode laser and the images of reflected light are captured by a CMOS sensor controlled by a PC via a USB interface. The refractive index resolution of $2.5x10^{-6}$ RIU for a 3% glycerol concentration is quite interesting but once again the device needs external processing capability. A further limitation lies in the coordination of the rotating mirrors, which requires a high synchronization between the frame rate of the image sensor and the revolution speed, so that it compromises the system's portability [21].

Monteiro et al. described another device based on Kretschmann's configuration in 2013. A semi-cylindrical prism is mounted on a rotary stage and irradiated by a laser beam. The samples are injected on a Teflon flow cell and an ad-hoc made CMOS detector performs the digital conversion of the acquired gray levels sending them to an external PC [22]. The sensitivity of the device was found to be 0.1573 mRIU per every pixel shift on the SPR curve, but once again this is not an autonomous system.

In the same year, Alvarez et al. designed a hybrid platform for the simultaneous detection of refractive index change and surface stress change [23]. The system is made up of a PMMA (Polymethyl methacrylate) microfluidic cell with two independent optical detection systems, one for the Krestchmam configuration and one for the measurement of a cantilever's optical deflection. Its detection limit is 5.5×10^{-5} RIU for a 0.1% ethanol solution. In this case, the control software is divided into two sections, one built into an on-board CPU and the other implemented on an external PC.

In addition to Kretschmann-based systems, diffraction grating techniques are used for the fabrication of compact biosensors. In 2009, Piliarik et al. presented a 4-channel compact biosensor made up of a miniaturized cartridge integrated with the diffraction grating and microfluidic apparatus [24]. The LED source beam is collimated so as to irradiate the cartridge and a CCD camera acquires the reflected signal.

In 2010, Vala et al. described an evolution of this device that can simultaneously detect 10 different analytes [25]. Despite the high sensitivity of both biosensors, about 10^{-7} RIU for a 0.00312 RI change, and the compact size, they are not autonomous systems because the processing requires a PC.

As we have illustrated in the previous section, in the last years a significant progress in nanotechnology has stimulated the study of Localized Surface Plasmon Resonance (LSPR) as an important solution to the problems posed by traditional SPR biosensors [26].

However, researchers' attention is mainly focused on the increase of sensitivity. Several works propose novel nanostructure fabrication techniques to identify the optimum nanoparticle configuration, shape, size, and material composition to obtain ultrasensitivity and selectivity for the target molecules [27-30].

Some of them integrated microfluidic platforms for specific research needs. For example, Geng et al. in 2014 described a LSPR sensor chip made up of an Au nanoparticles array integrated with microfluidics to detect liver cancer markers [31]. Hiep et al. in 2008 proposed an insulin and anti-insulin antibody detector based on a (polydimethylsiloxane) (PDMS) LSPR microfluidic chip [32].

Heider et al. in 2012 developed a gold nanorod substrate to quantify mercury in tap water [33] and a fiber-based biosensor utilizing the LSPR effect was developed by Lin et al. to evaluate the amount of organophosphorous pesticide [34].

All these devices need a spectrometer and an external PC to process data.

Few research works describe low-cost miniaturized LSPR devices, easy to produce, stand-alone, especially conceived for mass production.

For example, in 2011 Roche et al. proposed a low-cost LSPR platform that uses *camera phone* for diagnostic applications. The device is a steel cylinder housing RGB LEDs that irradiate a surface of nanoparticles. The camera phone acquires five images for each wavelength and transfers them by means of a microSD to an external laptop for *intensity* analysis [35]. Despite the low cost of the entire platform (20$ without the phone) and battery that can be recharged by solar power, the need for another device like a cellular phone and of an external PC to elaborate data limits its use in unfavorable

environments. A 2014 preliminary study by Dutta et al. also described the use of smartphone CCD cameras to create a low-cost evanescent wave coupled spectroscopic sensor [36].
Giavazzi et al. explore the same concept by developing a smartphone accessory to allow quick biosensing analysis [37]. Their detection method is based on an amorphous fluoropolymer substrate called Reflective Phantom Interface (RPI). This material has a refractive index close to that of an aqueous solution. Receptors immobilized on the substrate change the intensity of reflected light during their interaction with the corresponding antibodies.
The device is made up of the CCD camera of a phone, a LED source, a magnetic stirrer and a thermal stabilization system. The sensitivity of this instrumentation highly depends on the smartphone used, on the camera's resolution and on the compression algorithm implemented. A custom application running on the phone turns on the LED light and acquires images, but also in this case, the algorithm is processed by an external PC using a Matlab script. In addition, the power consumption of the telephone battery affects the device's efficiency during long time trials. This energy limitation is due to the several smartphone services employed at the same time: Wi-Fi or HSDPA connection, display refresh and other applications that must be active during the images' acquisition [38].
In 2013, Cappi et al. developed a portable transmission system that used a set of Fluorinated Tin Oxide-coated slides covered with *nano-islands* as sensing biochip. The biosensor measures the peak shift of the surface plasmon illuminating the sample with a LED source and acquires the reflected light signals by means of a photodiode [39]. The devices are equipped with a fan to reduce vibration and noise and to prevent the temperature from reaching excessively high values. However, the system's good resolution (the maximum peak deviation measured is about 0.9 nm), implies the use of a PC for elaborating the signals via LabVIEW code, and that prevents its portability.
In accordance with the state of the art described here, our research is focused on the development of a palm-size low-cost instrument that is easy to produce and can perform simultaneously multiple rapid assays outside research laboratories. In particular, we aimed at an autonomous, easy-to-use device, in which the analyses' results are immediately shown to the end-user without the use of an external PC.

IV. THE LSPRI BIOSENSOR SYSTEM

The device we propose [6], shown in figure 1a, is an EOT-based biosensor, 15 x 6 x 17 cm in size and less than 500g in weight, made up of a nanostructure biochip assembled on a custom cell with channels for the sample to flow through. A light source apparatus irradiates the chip surface and the electronic unit captures and elaborates the reflected light information.

A. Nanostructure array

Valsesia et al. developed the nanostructured biochip used in the prototype in 2011 [40]. Its sensitive surface consists of a nanohole array embedded in a continuous matrix of gold (fig. 1b). The chips were produced by means of a simple and well-known lithographic technique. A glass substrate was covered with plasma polymerized poly-acrylic acid (ppAA) by plasma enhanced chemical vapor deposition (PE-CVD). Then a layer of polystyrene beads (PS) was deposited on its top. A grating structure of regularly spaced pillars was realized by oxygen plasma etching. Finally, after a gold layer deposition using vapor to fill in the gaps between pillars, the residual PS mask was removed by lift-off in an ultrasonic bath of ultra-pure water. The crystal thus obtained features periodic gold cavities with a periodicity of 200 to 1000 nm with shapes that widen at the bottom (their opening width is in the range of 50-250 nm, their bottom width 100 to 450 nm) [40].
Studies on this kind of surface have revealed that this asymmetric pillar geometry increases the EOT effect in the cavities where the receptors are located, obtaining a biochip sensitivity in the order of 10^{-5} RIU [41].
Another peculiar feature is that the reflectance measured from the biochip glass side is sensitive to the refractive index at the opposite metal side. This allows measuring the optical response without complex optical platforms.

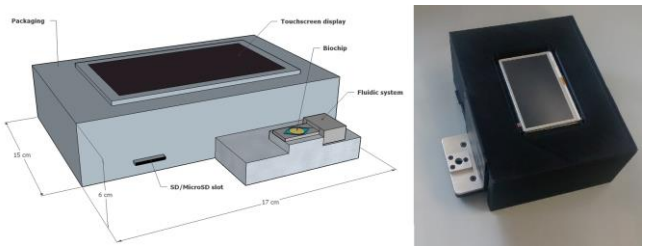

Fig. 1a. The biosensor prototype's external aspect (a draft and in the latest version).

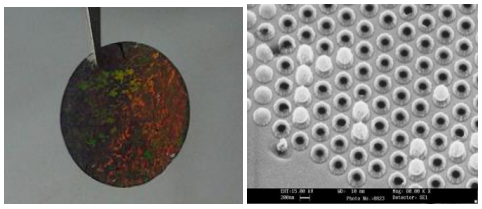

Fig. 1b. The biochip sensor and a nanohole array on a gold chip.

B. Optical apparatus

To maximize the response of the biochip's reflectance spectra to refractive index changes, we analyzed the surface's behavior under different wavelengths of light with a spectrometer. We identified in the 700-850 nm range the region where the SPR phenomenon occurs, so we selected an IR LED (Vishay TSHG8200) with a 830 nm wavelength peak as the light source for the trials.

The biochip is irradiated from the bottom (where it is wider) through an achromatic lens (AC127-025-b by Thorlabs Inc.) and a beamsplitter (CM1-BS015 by Thorlabs Inc.) that also

directs the light beam to the image detector (figure 2).

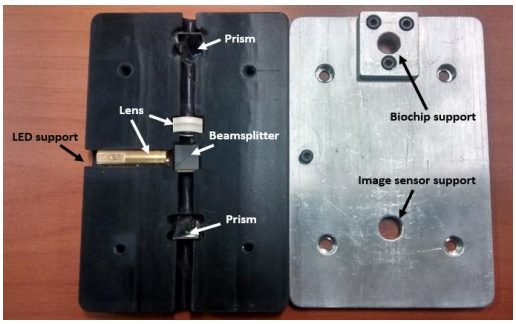

Fig. 2. Optical system details.

C. *Fluidics system*

A simple fluidic platform has been realized to perform all the sensitivity tests (figure 3). The system consists of a plexiglass cell divided into 2 channels, one for the solution injections and the other for baseline control. Each channel has specific intake and exhaust ducts for the solution to flow in, regulated by a peristaltic micropump.

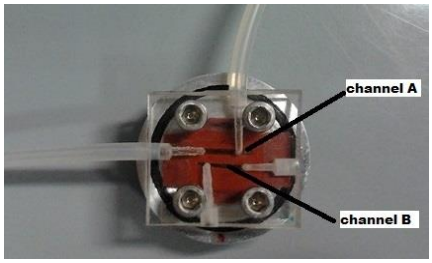

Fig. 3. Fluidics system with 2 sensing channels.

D. *Image processing unit*

Images are acquired by a ½-inch Active Pixel Sensor (APS) CMOS monochromatic digital image sensor.

APS CMOS sensors differ from the equivalent CCD for their lower cost, but they have a comparable sensitivity [42].

Our prototype included the CMOS MT9M001C12STM developed by Aptina Corporation, which has a quantum efficiency (QE) suitable for the required wavelength and a good resolution paired with low costs. In fact, its active area is made up of 1024x1280 pixels and each pixel is internally coded by an ADC in 10 bits grey levels.

The processing unit acquires large amounts of data from the sensor, processes them and sends them to a touchscreen display while storing all data and results into a MicroSD memory.

The management of these parts requires the careful choice of a suitable architecture. Studies on commercially available microcontroller families highlight the remarkable flexibility and high performance, combined with low cost and limited power consumption, of processors of the ARM family. In accordance with these premises, our prototype employs an ARM9 processor (AT91SAM9260 by Atmel Corporation) mounted on a SAM9-L9260 development board (Olimex Ltd). The board features a 64 MB SDRAM and a 512 MB Nand Flash, an 18.432 MHz oscillator, a RS232 interface, an Ethernet 100 Mbit controller and a SD/MMC card connector.

E. *Touchscreen display*

A 4.3" TFT 480x272 touch screen display integrated with an ARM Cortex-M4 LM4F232H5QD microcontroller was added. The user interface we developed allows the configuration of the biosensor's parameters for each assay and the real time monitoring of the kinetic reactions of the target substances.

Processed data are sent by the processing unit directly to the display processor, allowing the user to observe the trend of reactions divided by areas.

V. THE LAB-ON-CHIP INSTRUMENT

The lab-on-chip instrument we propose consists of a CCD image sensor, a SD memory for offline data analysis and a suitable touchscreen module and it is managed by an ARM 9 processor implementing a custom Linux kernel-based Operating System (Silly Switcher - SSW) [6], the simple monolithic Linux-based kernel, released under GNU General Public License (GPL) and based on the well-known *bootloader* U-boot.

We implemented a very light implementation of SSW featuring an MMU initialization (with 1 MB virtual memory), exceptions handlers, a simple I/O model, a module interface, and a task scheduler.

Each kernel module is initialized by means of an *initcall* request, which calls for a system boot, according to a specific hierarchy.

SSW uses static libraries techniques to extract only the modules needed for a specific application.

2 macros are used: *request()* and *provide()*. The former is called to request a specific module; the latter is called at the end of each module's source code.

In SSW each task of an application is implemented in a different way than in traditional Linux OS, using C functions that are invoked at each job instance. A Round Robin algorithm schedules all tasks, periodic and aperiodic. The task initialization function prepares the initial set up parameters like activation time and puts the task in a doubly linked list for idle tasks. Then, at job activation time, the task passes into another doubly linked list containing running tasks which can be extracted according to the Round Robin scheduling. The scheduler temporization is implemented using a timer that interrupts every 10 ms.

The SSW operating system also includes modules and drivers to manage biosensor components as shown in fig. 4.

This configuration is especially conceived to exploit simple GPIO pins for the interconnection of peripherals, with minimum hardware and software configuration effort, while assuring compatibility and flexibility with different systems.

Data transfer between the ARM9 and the touchscreen processor has been implemented through a specific SPI module. The interface running on the display processor is made up of three modules. The first one allows the user to initialize the biosensor, configure the assays' parameters (like

CMOS calibration, number of images to be acquired, etc.) and start each analysis. The second part reads the data processed by the processing unit and displays in real time the reaction's trend in a graph for each target substance. The user can obtain more details concerning the reaction directly from the trend chart. The third module displays the final report of the analysis: the substance concentrations that exceed a specified threshold are shown in red (figure 5). The thresholds for each target substance depend on the kind of analysis and on the type of receptors immobilized on the biochip.

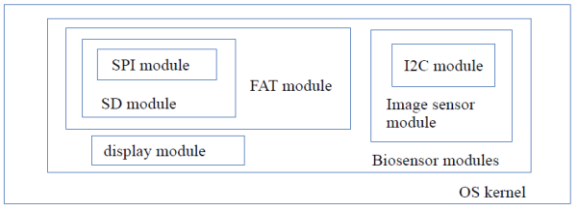

Fig. 4. Biosensor modules hierarchy.

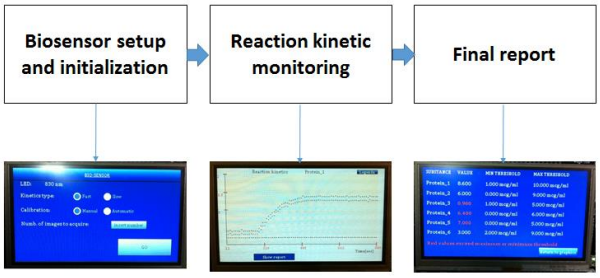

Fig. 5. The touchscreen application developed.

A MicroSD (or an SD) memory is provided to store all the acquired information and the analyses' results, receiving them from the main processor through an SPI bus.

The modules used for memory management are based on the three abstraction layers drown in figure 6; they manage the ARM registers' for SPI configuration, preserve compatibility with different SD types (standard SD, HCSD or XCSD) and implement a FAT 16 system to store assay parameters (number of captured images, processing time for each image, black level calibration, type of LED, analyte concentrations measured).

The MT9M001C12STM sensor consists of an active area of 6.66 mm x 5.32 mm made up by 1024 x 1280 pixels (10 bits grey level encoding).

Pixels readout during each frame acquisition is done on a row-by-row basis and controlled by signals provided by the sensor. Synchronization is achieved by means of a suitable external clock (1÷48 MHz).

A specific module has been developed for the initial sensor setup and readout configuration employing the I2C communication protocol. It allows the user to set scanning parameters, like reading modes of the pixel, black level calibration, duration of the blanking time, number of rows and columns to be considered.

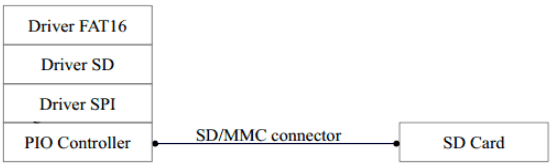

Fig. 6. Abstraction layers design for communication with the SD memory.

VI. Detection Algorithm

The biosensor software we developed configures the initial setup of the biosensor (with parameters such as the trials' periodicity and the number of images to be acquired), invokes the modules described above and provides the analyses' results.

We conceived specific algorithms for the acquisition of images using the GPIO processor interface via a simple PWM signal to provide a 2 MHz clock signal to the CMOS.

Each acquired image is immediately processed and stored into the SD memory in about 12 seconds.

A. Noise reduction

The detection and measurement of changes of refractive index requires an efficient algorithm that can provide the analyses' results quickly and accurately.

Studies on acquired data reveal that images are characterized by changes or fluctuations in light intensity.

In particular, the main effect observed is an upward trend of the pixels' grey level average during the trials that influences the analyses' results significantly (figure 7).

After 50 images, the light's intensity reaches a stable level.

The different saturation level observed with a 600 nm LED source is shown in figure 8 .

This behaviour is due to various factors, such as external temperature, light source wavelength, mechanical shocks, environmental noise, etc. However, experiments conducted with different black level calibrations, integration

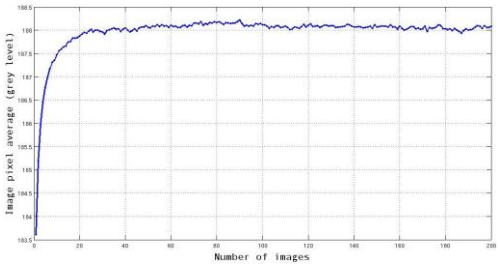

Fig. 7. Pixels' gray level average measured during the acquisition of 200 images without antibodies on the biochip surface. A 830 nm LED source was used.

times and LED sources, demonstrated that non-homogeneous light diffusion and photon accumulation on the sensor during long time expositions are the most significant causes of this phenomenon.

The study also revealed a saturation level that is not time-predictable, although each pixel undergoes the same brightness effects.

To overcome this instability we focused our attention on the identification of a not computationally heavy algorithm that could eliminate this drawback with quick response times and memory occupation.

The approach we adopted normalizes the pixels' grey level average of the sensitive area of the biochip where the antibodies are deposited with the average of an external area of the same surface without receptors defined as *control region*.

With this method, when the receptor-analyte reaction takes place, the different light intensity measured is influenced only by the LSPR phenomenon, without light aberrations.

To validate this approach, the biochip surface without immobilized antibodies is divided into three areas: two *control regions* and one selected region in which the solutions will be injected.

Figure 9 shows the pixel average ratios of three regions on the biochip surface. Two areas (2 and 3) are used as *control regions* and in the third distilled water is injected after acquiring 10 images.

The normalization we applied eliminates the instability described above and the ratios' values are constant before and after the water injection also within narrow areas.

Figure 9 also reveals that the variation of the pixel average ratios doesn't change if different regions are considered. This means that the measurement can be performed in different areas independently. All relevant information is included in the deviation from the baseline before and after the water injection, which corresponds to the refractive index change due to the LSPR phenomenon. This element is essential in order to identify the presence and the amount of an analyte in a sample.

The simple approach described here can also be easily extended to the final biochip configuration, with 2 control areas and an active area subdivided into micro-areas, one for each spot of receptors distributed along the surface.

The use of two control areas instead of one is an effective method to verify the measurements' accuracy, because it remains constant during all image acquisitions.

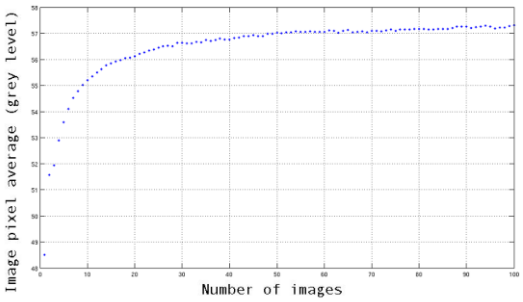

Fig. 8. Pixels' gray level average measured during the acquisition of 100 images without antibodies on the biochip surface. A 600 nm LED source was used.

B. *Data processing*

Once we had eliminated the instability of grey level average, we used the Time derivative of Pixel Average Ratio (abbreviated in TdPAR) to evaluate the refractive index change on the biochip's surface.

In particular, we considered the difference between the ratio values measured during the previous and the current acquisition.

Fig. 10 shows the trend of the three areas' average ratios and the time derivatives of two control regions (area 1 and area 2) and a sample area (area 3), each one of 128x128 pixels. Distilled water was used as the reference baseline, then (after acquiring 14 images) a 5% glycerol solution was injected on the sample area.

Just as in the previous case, we observed a change in the measured ratios corresponding to the glycerol injection and the peak's position corresponds to the refractive index's variation.

The algorithm uses the amplitude of the peak to define the target analyte's concentration by comparing it with a specific refractive index calibration table stored in the internal memory of the processor.

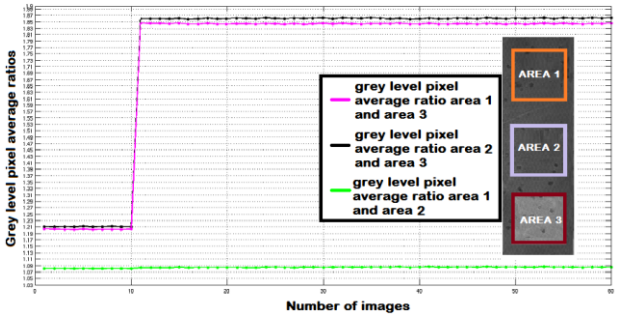

Fig. 9. Pixels' average gray level ratios measured during the acquisition of 60 images without antibodies on the biochip surface. A 830 nm LED source was used. 128x128 pixels areas were used for the experiment. Areas 1 and 2 are control regions.

C. *Sensitivity curve*

The biosensor's sensitivity to bulk refractive index changes was defined using a set of glycerol solutions with different concentrations (0.2% ÷ 5%).

As already mentioned, the fluidics system employed consists of 2 channels (fig. 3). The first channel was used as reference, the second one as active area. The images of the channels acquired were divided into three rectangular areas (150x800 pixels), two corresponding to the control channel and one to where the solutions were injected.

Distilled water was made to flow into the second channel as a stable baseline for a small number of images (5-10) and then the glycerol solution was introduced. The acquisition session for each concentration took less than 30 minutes.

Fig. 11 shows the relation between the peak amplitude of the time derivative of the pixels' average gray level ratio and the refractive index corresponding to specific glycerol solutions (0.2%, 0.5%, 1%, 2%, 3%, 4%, 5%).

The corresponding refractive index of the solutions and of distilled water was measured with an Abbe refractometer (10^{-4} RIU resolution).

Each experiment was repeated three times to ensure the measurements' repeatability and the pixel average values were

filtered with a simple moving average filter so as to avoid affecting the processing time significantly and to obtain a real time response.

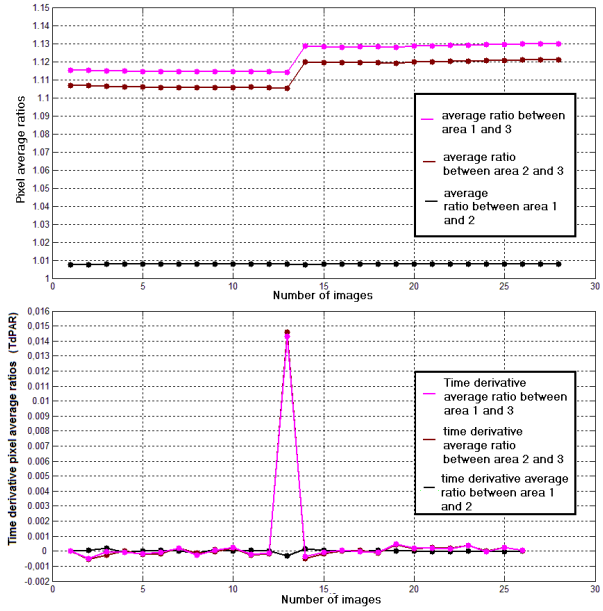

Fig 10. Pixel average ratio and time derivative (TdPAR) trends when sample area 3 is filled with distilled water (refraction index = 1.333) and then with a 5% glycerol solution (refraction index = 1.339) [6].

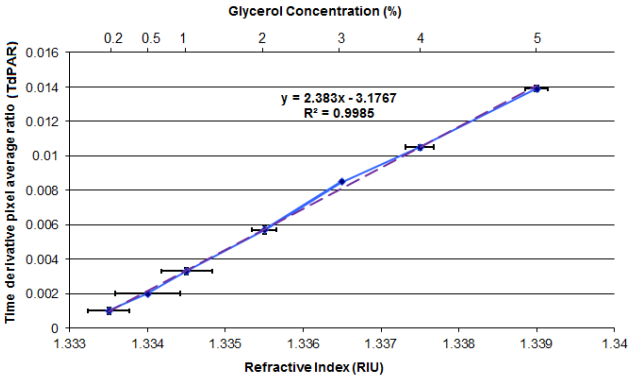

Fig 11. Trend of TdPAR vs. refractive index associated with different glycerol concentrations. Distilled water (n = 1,333) was assumed as reference.

The analytical curve of the time derivative measured shows a good linearity to the change of refractive index.

The correlation coefficient (R^2) of standard y-intercept and measured data was 0.9985.

On the basis of the refractive index calibration the biosensor's sensitivity was determined to be 2.383 TdPAR/RIU.

The standard deviation of the baseline noise was 1.59 x 10^{-4} TdPAR, which corresponds to a refractive index resolution of 6x10^{-5} RIU. This result confirmed the theoretical detection limit of the biochip studied in [41] and it is sufficient in many biosensing applications.

The response variation with respect to the standard intercept is caused by various factors. The CMOS image sensor parameters, such as black level calibration, and properties, such as the quantum efficiency at the wavelength employed, may cause statistical fluctuations in the quantity of light captured.

VII. Antigen-Antibody Binding Detection

For biosensing measurements, the Pentraxin-related protein (PTX3) was used to evaluate the effective "in vivo" detection capability of our portable system. In particular, two SPR chips have been functionalized to perform the immobilization of PTX3.

A bath of MHD (Mercaptohexadecanoic acid) in an Ethanol solution at 5 mM was used to prepare the chips' surface. Then a mix of standard 1-Ethyl-3 (dimethylaminopropyl) carbodiimide/N-Hydroxysuccinimide (EDC/NHS) was injected to activate the COOH covalent bindings for the protein immobilization.

After the solution was washed out and the chip dried, the surface was divided into two regions: one, the active area, loaded with PTX3 (100 μg/ml) and one to be used as control.

PTX3 was purified by immunoaffinity from the supernatant of transfected Chinese hamster ovary cells.

After a 2-hours incubation, a bath of ethanolamine (pH 8.5) with PBS and a dilution of BSA deactivated the COOH groups and passivated the control area.

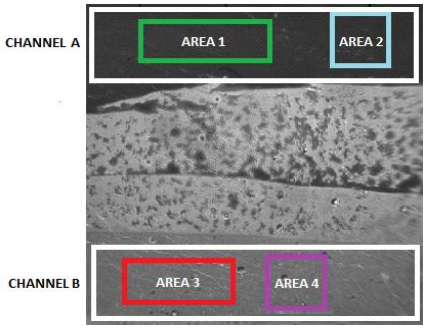

Fig. 12. Different pixel regions on the chip surface. Area 1 (300x100 pixels) and area 2 (128x128) are located in correspondence with channel A. Area 3 (250x100) and area 4 (128x128) are located in correspondence with channel B.

A. *Experiments*

The microfluidics system shown in fig. 3 was used to perform the trials. Channel A adheres to the control region of the chip and channel B to the active area. A peristaltic micro pump (38 μl/min) filled the active area with the liquid sample. First, a PBS solution was made to flow in channel B as a stable reference baseline, and then the antibody raised against the PTX3 (Ab-PTX3) was introduced (10 µg/ml in a 10 mM acetate buffer with pH 5). After that, the channel was rinsed with the PBS solution.

The detection algorithm was applied to 4 pixel regions of the images captured by the CMOS sensor to evaluate the response in different areas of every channel (fig. 12).

Figure 13 shows the change of pixel average ratio during a 30 minutes trial, in accordance with the trend of the reaction kinetics of the PTX3 antibodies on the chip surface.

B. *Analytes recognition*

The protein molecules' physical adsorption onto the biochip active area shows a generalized trend, independent of the pixel regions used.

As shown in figure 13, when the PBS solution rinse was used after the Ab-PTX3 solution to remove unbound molecules, the Ab-PTX3 molecules immobilized by the PTX3 on the surface were stable and homogenous. This demonstrates the high receptor-analyte affinity and indicates the correct recognition of the antibody.

The variation of the ratios observed after the injection is about two orders of magnitude greater than the reference baseline (PBS solution).

The time derivative measured is ~5 x 10^{-2} TdPAR, which corresponds to 1.354 RIU with a baseline standard deviation of ~1 x 10^{-4} TdPAR, for both chips used.

The tests performed show the antibody detection capability of the instrument. A recent study [43] hypothesizes a correlation between the presence of Ab-PTX3 and systemic lupus erythematosus. When this hypothesis will be definitively confirmed, the instrument will be of great help also in the early medical diagnosis of this pathology.

Finally this kind of rapid analysis (it takes less than 30 min) allows medical doctors to act promptly without waiting for lab analyses.

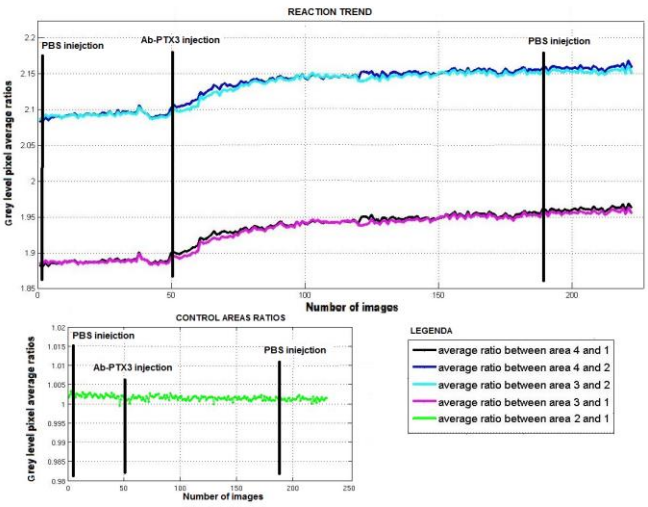

Fig. 13. Pixels' average gray level ratios measured during the acquisition of 230 images. A 830 nm LED source was used. The antibody injection takes place after the 50th image's acquisition, then at the 187th's a PBS solution was injected into the channel.

VIII. Conclusions

The SPR technique has been used for several years to detect and monitor changes in the refractive index on a metal surface. However, almost all of the commercially available SPR biosensors are expensive and unsuitable for use outside of laboratories due to their size. Many research activities involving the use of nanostructured surfaces have been aimed at overcoming this limitation; however, the development of autonomous, portable and sensitive instrumentations is still an underestimated problem [44].

In this paper, we presented a new embedded, compact and low cost lab-on chip unit made up of an LSPR biosensor equipped with a detection unit for a multiparametric analysis of complex chemical and biological samples.

An existing platform using the same biochip technology is illustrated by [45]; it consists of a label-free imaging system called Imaging Nanoplasmonics™. The instrument's weight is not negligible (6 Kg) and its lunch box size further threatens its portability; moreover it's more expensive than the one described here.

The product of our research differs from this device because it is a novel biosensor especially conceived to be portable (a palm-size device of 17x15x6 cm size and less than 500g weight), and fit to be used for in loco analyses without laboratory support. Of course we still need to take several steps before our research reaches final applicability, i. e. the biochip nanohole array surface should be optimized, its response to real human biological fluids (serum/blood) investigated, its duration and long-term stability checked. However its potential applicability can already be foreseen.

For example, in rural locations or in developing countries, it could be used to monitor patients' biological parameters, for the detection of infectious diseases or for blood tests. In the field of agrifood, it could be used for the detection of contaminants in water and food and in the pharmaceutical and industrial fields for the control of chemical processes.

The device captures images from a nanohole array biochip, irradiated by an IR LED at a 830 nm wavelength. More than 100 microspots of antibodies which are sensitive to the different molecules to be searched can be deposited on the biochip's metal surface. If the chemical reaction takes place, the change in the refractive index can be measured thanks to the variation in the reflected light's intensity. This information is acquired by a monochrome CMOS image sensor and processed by a processor of the ARM9 family.

The heart of the instrument lies in the specifically conceived management software running on Linux-based operating systems. This software platform that runs on the embedded processor consists of specific communication modules and of a suitably tuned analyte detection algorithm.

The modules we designed don't require a specific interface to be already integrated into the processor, but only a GPIO interface. This feature makes this platform suitable also for other processors of the ARM family.

The detection algorithm we developed extracts the relevant data from the acquired images by removing the noise effects due to external environmental conditions and internal CMOS characteristics using the time derivative of the pixels' average ratios.

The device we propose is completely autonomous and its analyses' results are made immediately available on a touchscreen display and stored into an external SD memory in about 12 seconds.

Its power consumption is about 2.38 W (475 mA x 5 V), due mainly to the ARM development board. The touchscreen display is powered by a separate 3.7 V Li-Polymer battery. A

significant reduction of these values is expected by the time the final system will be ready for the market.

The prototype's cost is estimated at less than € 600 and it can be used also by untrained personnel. This is a significant reduction in costs if we consider that similar devices are today available but their costs exceed ten and even a hundred thousand Euros (see Tab. 1).

The instrument's sensitivity to bulk refractive index changes has also been measured. The resolution obtained for different glycerol solutions is about 6 x 10^{-5} RIU, a result that is suitable in several applications and consistent with the biochip theoretical studies shown in [41].

The performances of the device we propose for rapid diagnostic have been described in the previous section. The trials demonstrated the device's sensing capability in detecting the level of the pentraxin PTX3 antibody, potentially useful in clinical diagnostics to reveal existing diseases and autoimmune pathologies [43].

The device's peculiar characteristics and the results we obtained confirm the strong potential of the prototype in a wide range of fields, especially for those world areas where it is not possible or it is very difficult to perform this type of analyses.

We are aware that the proposed technology can be considered in direct competition or as an alternative to smartphone based Point of Care diagnostics. In [53] a very complete overview of this approach is presented covering several "in vivo" and "in vitro" applications. We feel that this could be a consistent and promising possibility for the future, assuming to overcome present limitations related to security or confidentiality and to usability from elderly people, untrained operators or persons with temporal and permanent disabilities.

The next steps of the project will improve the instrument's usability both by reducing its weight and size and by equipping it with a suitable Wi-Fi module to communicate the analyses' results.

ACKNOWLEDGMENTS

The authors are very thankful to prof. Alessandro Rubini for his invaluable help and support during the development of the SSW operating system and the ARM9 modules. This project is carried out in collaboration with Plasmore S.r.l., the Joint Research Centre European Commission (JCR) of Ispra (Varese, Italy), the Electrical, Computer and Biomedical Engineering department and the Physics department "A. Volta", both part of the University of Pavia. Plasmore and JCR were involved in the design and realization of the nanostructured biochip, the Physics department was responsible for the optical setup. Many thanks to Andrea Valsesia and Lucia Fornasari for their useful advices.

REFERENCES

[1] Byun K. M., "Development of nanostructured plasmonic substrates for enhanced optical biosensing", *J. Opt. Soc. Kor*., 2010, No. 2, Vol. 14, pp. 65-76.

[2] Huang C., Bonroy K., Reekmans G., Laureyn W., Verhaegen K., De Vlaminck I., Lagae L., Borghs G., "Localized surface plasmon resonance biosensor integrated with microfluidic chip", Biomed. Microdevices, 2009, Vol. 11, pp. 893-901.

[3] Malic L., Veres T., Tabrizian M., "Nanostructured digital microfluidics for enhanced surface plasmon resonance imaging", *Biosensors and Bioelectronics*, 2011, Vol. 26 (5), pp. 2053-2059.

[4] Wei J.J., Rexius M., Kofke M., Wang Y., Singhal S., Waldeck D. H., "Nano-plasmonics Sensing and Integration with Microfluidics for Lab-on-chip Biosensor", Nanotechnology, 2011, Vol. 3, pp. 79-82.

[5] Geng Z. X., Kan Q., Yuan J., Gao H. S., Wang C. X., Chen H. D., "Mass-producible low-cost Au nanostructure nanoplasmonic biosensor on optofluidic-portable platform", Transducer 2013, Barcelona, Spain, 16-20 June 2013, pp. 2435-2438.

[6] S. Rampazzi, F. Leporati, G. Danese, N. Nazzicari, L. Fornasari, F. Marabelli, A. Valsesia, "A Novel Portable Surface Plasmon Resonance Based Imaging Instrument for On-Site Multi-Analyte Detection", FedCSIS Federated Conference on Computer Science and Information Systems, Kraków, Poland, September 8-11, 2013, pp. 619-626.

[7] Mayer K. M., Hafner J. H., "Localized Surface Plasmon Resonance Sensors", *Chemical Reviews*, 2011, Vol. 111, pp. 3828-3857.

[8] Yuk J. S., Jung J-W., Jung S-H., Han J-H., Kim Y-M., Ha K-S., "Sensitivity of ex situ and in situ spectral surface plasmon resonance sensors in the analysis of protein arrays", *Biosensors and Biolectronics*, 2005, Vol. 20, pp. 2189-2196.

[9] Roh S., Chung T., Lee B., "Overview of the Characteristics of Micro- and Nano-Structured Surface Plasmon Resonance Sensors", *Sensors*, 2011, No. 11, pp. 1565-1588.

Product	Cost ($)	Size (cm)	Weight (Kg)	Resolution (RIU)	N° of channels	Stand-alone
Biacore T200 [46]	386.958	60 x 61,5 x 69	60	10^{-8}	4	No
Autolab ESPRIT[47]	97.500	60 x 51 x 45	40	10^{-5}	2	No
SensiQ Pioneer[48]	180.000	60 x 57 x 50	30	0,25 x 10^{-6}	2	No
ProteOn XPR-36[49]	285.000	95 x 58 x 50	85	10^{-6}	6 x 6	No
Reichert SR7500DC[50]	95.000	39,4 x 32 x 14	25	0,05 x 10^{-6}	2	No
OpenSPR[51]	14.995	16 x 21 x 12	5	10^{-4} -10^{-5}	1	No
SPIRIT[52]	35.000	28 x 22 x 13	3	10^{-5} -10^{-6}	12	Yes
Our system	< 700	17 x 15 x 6	0.5	6 x 10^{-5}	2	Yes

Tab 1. A comparison between our device and commercially available instruments (portable and not).

[10] Velasco-Garcia M. N., "Optical biosensor for probing at the cellular level: A review of recent progress and future prospects", *Seminars in Cell & Developmental Biology*, 2009, Vol. 20, pp. 27-30.

[11] Zalyubovskiy S. J., Bogdanova M., Deinega A., Lozovik Y., Pris A. D., Hyup An K., Hall W. P., Potyrailo A., "Theoretical limit of localized surface plasmon resonance sensitivity to local refractive index change and its comparison to conventional surface plasmon resonance sensor", *Journal of the Optical Society of America*, 2012, Vol. 29, No. 6, pp. 994-1002.

[12] Chiang H. P., Chen C. W., Wu J. J., Li H. L., Lin T. Y., Sánchez E. J., Leung P. T., "Effects of temperature on the surface plasmon resonance at a metal-semiconductor interface", *Thin Solid Films*, 2007, Vol. 515, pp. 6953-6961.

[13] Lopatynskyi A. M., Lopatynska O. G., Guo L. J., Chegel V. I., "Localized Surface Plasmon Resonance Biosensor – Part 1: Theoretical Study of Sensitivity – Extended Mie Approach", *IEEE Sensors Journal*, 2011, Vol. 11, No. 2, pp. 361-369.

[14] Petryayeva E., Krull U. J., "Localized surface plasmon resonance: Nanostructures, bioassays and biosensing - A review", *Analytica Chimica Acta*, 2011, Vol. 706, pp. 8-24.

[15] Ebbesen T. W., Lezec H. J., Ghaemi H. F., Thio T., Wolff P.A., "Extraordinary optical transmission through subwavelength hole arrays", Letters to Nature, 1998, Vol. 391, pp. 667-669.

[16] Chinowsky T. M., Quinn J.G., Bartholomew D.U., Kaiser R., Elkind J.L., "Performance of the Spreeta 2000 integrated surface plasmon resonance affinity sensor", *Sensors and Actuators B: Chemical*, 2003, No. 91, pp. 266-274.

[17] Koel M., Kaljurand M., "Green Analytical Chemistry", 2010, RSC Publishing, ISBN: 978-1-84755-872-5.

[18] Chinowsky T. M., Soelberg S. D., Baker P., Swanson N. R., Kauffman P., Mactutis A., Grow M. S., Atmar R., Yee S. S., Furlong C. E., "Portable 24-analyte surface plasmon resonance instruments for rapid, versatile biodetection", *Biosensors and Biolectronics*, 2007, Vol. 22, pp. 2268-2275.

[19] Hu J., Hu J., Luo F., Li W., Jiang G., Li Z., Zhang R., "Design and validation of a low cost surface plasmon resonance bioanalyzer using microprocessors and a touch-screen monitor", *Biosensors and Bioelectronics*, 2009, Vol. 24, pp. 1974-1978.

[20] Cai H., Li H., Zhang L., Chen X., Cui D., "Portable Surface Plasmon Resonance Instrument based on a Monolithic Scanner Chip", 3rd International Conference on Biomedical Engineering and Informatics, Yantai, China, 16-18 October 2010, pp. 1153-1155.

[21] Shin Y.-B., Min Kim H., Jung Y., Chung B.H., "A new palm-sized surface plasmon resonance (SPR) biosensor based on modulation of light source by rotating mirror", *Sensors and Actuators B: Chemical*, 2010, No. 150, pp.1-6.

[22] Montero J. I., Mukherji S., Kundo T., "Development of a low-cost portable Surface Plasmon Resonance biosensor", International Conference on Microelectronics, Communication and Renewable Energy (ICMiCR-2013), Kanjirapally, June 2013, pp. 1-5.

[23] Alvarez M., Fariña David, Escuela A. M., Ramón Sendra, Lechuga L. M., "Development of a surface plasmon resonance and nanomechanical biosensing hybrid platform for multiparametric reading", *Review of Scientific Instruments*, 2013, Vol. 84, pp. 1-8.

[24] Piliarik M., Vala M., Tichý I., Homola J., "Compact and low-cost biosensor based on novel approach to spectroscopy of surface plasmons", *Biosensors and Biolectronics*, 2009, Vol. 24, pp. 3430-3435.

[25] Vala M., Chadt K., Piliarik M., Homola J., "High-performance compact SPR sensor for multi-analyte sensing", *Sensors and Actuators B: Chemical*, 2010, No. 148, pp. 544-549.

[26] Wijaya E., Lenaerts C., Maricot S., Hastanin J., Habraken S., Vilcot J., Boukherroub, Szunerts S., "Surface plasmon resonance-based biosensors: From the development of different SPR structures to novel surface functionalization strategies", *Current Opinion in Solid State and Materials Science*, 2011, Vol. 15, pp. 208-224.

[27] Armelles G., González-Díaz J. B., García-Martín A., García-Martín J. M., Cebollada A., Ujué González M., Acimovic S., Quidant J. C. R., Badenes G., "Localized surface plasmon resonance effects on the magneto-optical activity of continuous Au/Co/Au trilayers", *Optics Express*, 2008, Vol. 16, Is. 20, pp. 16104-16112.

[28] Zhang S., Bao K., Halas N. J., Xu H., Nordlander P., "Substrate-Induced Fano Resonances of a Plasmonic Nanocube: A Route to Increased-Sensitivity Localized Surface Plasmon Resonance Sensors Revealed", *Nano Letters*, 2011, Vol.11, Is. 4, pp. 1657-1663.

[29] Verellen N., Van Dorpe P., Huang C., Lodewijks K., Vandenbosch G. A. E., Lagae L., Moshchalkov V. V., "Plasmon Line Shaping Using Nanocrosses for High Sensitivity Localized Surface Plasmon Resonance Sensing", *Nano Letters*, 2011, Vol.11, Is. 2, pp. 391-397.

[30] Lish K. P., Pradeep T., "Enhanced visual detection of pesticides using gold nanoparticles", *Journal of Environmental Science and Health, Part B: Pesticides, Food Contaminants, and Agricultural Wastes*, 2009, Vol. 44, pp. 697-705.

[31] Geng Z., Kan Q., Yuan J., Chen H., "A route to low-cost nanoplasmonic biosensor integrated with optofluidic-portable platform", *Sensors and Actuators B: Chemical*, 2014, Vol. 195, pp. 682-691.

[32] Hiep H. M., Nakayama T., Saito M., Yamamura S., Takamura Y, Tamiya E., "A Microfluidic Chip Based on Localized Surface Plasmon Resonance for Real-Time Monitoring of Antigen–Antibody Reactions", *Japanese Journal of Applied Physics*, 2008, Vol. 47, No. 2S, p. 1337-1341.

[33] Heider E. C., Trieu K., Moore F. T., Campiglia A. D., "Portable mercury sensor for tap water using surface plasmon resonance of immobilized gold nanorods", *Talanta*, 2012, Vol. 99, pp. 180-185.

[34] Lin T-J., Huang K-T., Liu C-Y., "Determination of organophosphorous pesticides by a novel biosensor based on localized surface plasmon resonance", *Biosensors and Bioelectronics*, 2006, Vol. 22, pp. 513–518

[35] Roche P. J. R., Filion-Côtè S., Cheung C.-K., Chodavarapu V. P., Kirk A. G., "A Camera Phone Localized Surface Plasmon Biosensing Platform towards Low-Cost Label-Free Diagnostic Testing", *Journal of Sensors*, 2011, Vol. 2011, pp.1-7.

[36] Dutta S., Choudhury A., Nath P., "Evanescent Wave Coupled Spectroscopic Sensing Using Smartphone", *IEEE Photonics Technology Letters*, 2014, pp. 1041-1135

[37] Giavazzi F., Salina M., Ceccarello E., Ilaqua A., Damni F., Sola L., Chiari M., Chini B., Cerbino R., Bellini T., Buscaglia M., "A fast and simple label-free immunoassay based on a smartphone", *Biosensors and Bioelectronics*, 2014, Vol. 58, pp. 395-402.

[38] Perrucci G. P., Fitzek F. H. P., Widmer J., "Survey on Energy Consumption Entities on the Smartphone Platform", Vehicular Technology Conference (VTC Spring), Yokohama (Japan), May 15-18, 2011, pp.1-6.

[39] Cappi G., Accastelli E., Cantale V., Rampi M. A., Benini L., Guiducci C., "Peak shift measurement of localized surface plasmon resonance by a portable electronic system", *Sensors and Actuators B: Chemical*, 2013, Vol. 176, pp. 225-231.

[40] Valsesia et al., 2013, "SPR sensor device with nanostructure", European Patent Application 11174058.5, 16/01/2013.

[41] Giudicatti S., Valsesia A., Marabelli F., Colpo P., Rossi F., "Plasmonic resonance in nanostructured gold/polymer surfaces by colloidal lithography", *Physica Status Solidi A*, 2010, Vol. 207, No. 4, pp. 935-942.

[42] Carlson, B.S., "Comparison of modern CCD and CMOS image sensor technologies and systems for low resolution imaging", *Sensors. Proceedings of IEEE*, 2002, Vol.1, pp. 171- 176.

[43] Augusto J-F., Onno C., Blanchard S., Dubuquoi S., Mantovani A., Chevailler A., Jeannin P., Subra J-F., "Detection of anti-PTX3

autoantibodies in systemic lupus erythematosus, *Rheumatology*, 2009, Vol. 48 (4), pp. 442-444.

[44] D'Orazio P., "Biosensors in clinical chemistry - 2011 update", *Clinica Chimica Acta*, 2011, Vol. 412, pp. 1749-1761.

[45] Bottazzi B., Fornasari L., Frangolho A., Giudicatti S., Mantovani A., Marabelli F., Marchesini G., Pellacani P., Theisod R., Valsesia A., "Multiplexed label-free optical biosensor for medical diagnostics", *Journal of Biomedical Optics*, 2014, Vol. 19, No. 1, pp. 1-10.

[46] GE Healthcare, "Outstanding sensitivity for confident label-free interaction analysis", 28-9794-20 AA 06/2010, 2010.

[47] Metrohm Siam Ltd., "Autolab ESPRIT Data Acquisition 4.4 User manual SPR", 08/2009.

[48] Nomadics Inc., "SensiQ – Techical Overview", 2007.

[49] Bio-Rad Laboratories Inc., "Protein interaction Analysis ProteOn™ XPR36 Hardware", Bulletin 5413, 2007.

[50] Reichert Technologies, "SR7500DC Dual Channel Surface Plasmon Resonance System", 10/11-BP-Qty: 3000, 2011.

[51] Nicoya Lifesciences, "OpenSPR Nanoscale molecular analysis on your benchtop", 2014.

[52] Seattle Sensor System Corporation, "SPIRIT-Portable SPR Instrument Specifications", SSS-SPIRIT-V4.0, April 2012.

[53] Xiayu Xu; Akay, A.; Huilin Wei; ShuQi Wang; Pingguan-Murphy, B.; Erlandsson, B.-E.; XiuJun Li; WonGu Lee; Jie Hu; Lin Wang; Feng Xu, "Advances in Smartphone based Point of Care Diagnostics", Proceedings of the IEEE, vol. 103, n° 2, February 2015, pp. 236-247.

Sara Rampazzi received the M.S. and PhD degrees in Computer Engineering at University of Pavia (Italy) in 2010 and 2014, respectively. She was Research Fellow with the Department of Electrical, Computer and Biomedical Engineering from 2014 to 2015. Her research concerned computer and microprocessor architectures, embedded systems, image sensors and biomedical instrumentations. In 2014 she was visiting researcher at IUMA (Istituto Universitario de Microelectronica Aplicada) at the University of Las Palmas de Gran Canaria (Spain) where she worked on parallel architectures for hyperspectral image processing. She is currently a Model Based Design engineer with R&D Division, Magneti Marelli S.p.A., (Corbetta, Italy). Contact her at sara.rampazzi@gmail.com

Giovanni Danese was born in Maglie (Lecce) on June 12th, 1956. In 1981 he tooks his degree summa cum laude and in 1987 his PhD degree in Electronics and Computer Engineering. Since 1989 until 1992 he was assistant professor in the Engineering Faculty of the University of Pavia; on 1992 he became Associate Professor in the field of the Computer Engineering. On 2001 he became full professor of Computer Programming and Computer Architecture with the Department of Electrical, Computer and Biomedical Engineering at the University of Pavia. His current research interests include parallel computing, special-purpose computers, and signal and image processing. He is a member of the IEEE and received awards for his researches and he was invited speaker in international conferences.

Francesco Leporati is associate professor of Industrial Informatics and Digital Systems Design with the Department of Electrical, Computer and Biomedical Engineering at the University of Pavia. His current research interests include automotive applications, FPGA and application-specific processors, embedded real-time systems, computational physics. Leporati has a PHD in electronics and computer engineering from the University of Pavia. He is a member of the IEEE and Euromicro societies.

Franco Marabelli was born in 1959, PhD at the Swiss Federal Institute of Technology (ETH)Zurich, and since 2011 is full professor at the Physics Department of the University of Pavia.
His main interest is the optical spectroscopy of solid state materials and he has been involved in researches on heavy fermions, silicides and fullerenes and SiGe systems. The recent topic of interest are photonic crystals and optical response in semiconducting polymers. In collaboration with the Joint Research Centre of the European Commission in Ispra, he began the study of biosensor devices based on plasmonic crystals. Such a work leads to some patents and a spin off.